Metrol. Meas. Syst., Vol. 29 (2022), No. 1
DOI: 10.24425/mms.2022.138545

METROLOGY AND MEASUREMENT SYSTEMS
Index 330930, ISSN 0860-8229
www.metrology.wat.edu.pl

ANALYSIS, EVALUATION, AND OPTIMIZATION OF BIO-MEDICAL THERMO-RESISTIVE MICRO-CALORIMETRIC FLOW SENSOR USING AN ANALYTICAL APPROACH

Mojtaba Babaelahi[1)], Somayyeh Sadri[2)]

1) *Department of Mechanical Engineering, University of Qom, Qom, Iran* (✉ *m.babaelahi@qom.ac.ir*)
2) *Thermal Cycle and Heat Exchangers Department, Niroo Research Institute, Tehran, Iran* (*ssadri@nri.ac.ir*)

Abstract

The sensitive MEMS-based thermal flow sensors are the best choice for monitoring the patient's respiration to prompt diagnosis of breath disturbances. In this paper, the open space micro-calorimetric flow sensors are investigated as precise monitoring tools. The differential energy balance equation, including convection and conduction terms, is derived for the thermal analysis of the considered sensor. The temperature-dependent thermal conductivity of the silicon-oxide membrane thin layer is considered in the energy balance equation. The derived thermal non-linear differential equation is solved using a well-known analytical method, and a finite-element numerical solution is used for the confirmation. Results show that the presented analytical model present precise tools for evaluating these sensors. The effects of flow and membrane thin film parameters on thermo-resistive micro-calorimetric flow sensors' performance and sensitivity are evaluated. The optimization has been performed at different flow velocities using a genetic algorithm method to determine the optimum configuration of the considered flow sensor. The geometrical parameters are selected as a decision variable in the optimization procedure. In the final step, using optimization results and curve-fitting, the expressions for the optimum decision variables have been derived. The sensor's optimum configuration can be achieved analytically based on flow velocity with the analytical terms for optimum decision variables.

Keywords: thermo-resistive, micro-calorimetric, sensor, temperature, variable conductivity, analytical solution, optimization.

1. Introduction

The fluid flow measurement is one of the essential tools for analyzing various systems. Therefore, the accuracy of fluid flow measuring instruments is crucial and has been considered by various researchers. One of the conventional fluid flow measuring tools is microflow sensors divided into thermal and non-thermal categories. The thermal flow sensors category shows great applicability in microfluidic devices, medical ventilation, spacecraft propulsion systems, and environmental monitoring. It has three sub-categories: hot wire/hot film, calorimetric, and flight time [1,2].

Prompt diagnosis of breath disturbances is one of the essential requirements and preconditions of the treatment procedure. Performing this medical diagnosis requires monitoring the patient's respiration, and this monitoring requires appropriate sensors. The best choice is a sensitive MEMS-based thermal flow sensor with a fast response time (1 kHz) and low power consumption. Micro-fabricated devices' valuable characteristics such as high sensitivity, accuracy and precision, low power consumption, and small size have provided a better patient outcome and lower healthcare costs. Most applications of these sensors are in measuring physical parameters such as flow pressure. These sensors' usage monitors blood

Article history: received August 11, 2021; revised September 20, 2021; accepted September 23, 2021; available online November 9, 2021.

flow, pressure measurement (such as intravascular blood pressure), microsurgery, bladder, cerebrospinal fluid pressure measurement, and drug delivery [3]. Different researches have been performed on modeling, designing, manufacturing, and optimizing fluid flow measurement tools. Some of these researches are considered in the flowing section.

Wei *et al.* [1] presented a simple one-dimensional analytical model for a *thermo-resistive micro calorimetric flow* (TMCF) sensor. They used the CFD simulations and experimental data to validate the model and studied the effect of key design parameters on the sensor performance. Wei *et al.* [2] presented a theoretical and experimental investigation on TMCF sensors Fabricated by CMOS MEMS Technology. They analyzed a general one-dimensional model to predict the TMCF sensor characteristics with two packagings, *i.e.*, channel and open-space types. They optimized the TMCF sensor's design by scaling the sensor output, sensitivity, and power consumption value. They designed and fabricated three TMCF sensors by using a 0.35 μm 2P4M CMOS microelectromechanical systems technology. Ferdous *et al.* [4] optimized a micro-machined thermal flow rate sensor. They tried to achieve high sensitivity and low power consumption by employing a large thermal conductivity substrate. They found that the sensor has a more considerable sensitivity in the velocity range up to 1 m/s. Wei *et al.* [5] analyzed a wafer-level encapsulated *Thermo-Resistive Micro Calorimetric Flow* (TMCF) sensor. For the fluid, nitrogen gas was selected. They achieved a normalized sensitivity of 112.4 mV/ (m/s)/mW for pulsed operated TMCF sensor under constant temperature difference mode. They concluded that the sensors could be used for IoT technology in smart buildings. Wei *et al.* [6] proposed a new one-dimensional TMCF sensor model for moist airflow with temperature-dependent thermophysical properties. They fabricated a sensor with a superior sensitivity of 0.543 V/(m/s). Franz *et al.* [7] analyzed micro machined calorimetric flow sensors by FEM simulations. Dumstorff *et al*. [8] presented a novel packaging method to analyze a membrane-based thermal flow sensor. To avoid turbulence or reduce channel cross-section or sensitivity, they placed a flow sensor in a channel in different step arrangements. Arpys *et al.* [9] used COMSOL Multi-physics to simulate a thermal transport-based flow sensor. They found that the maximum temperature difference between the two temperature sensors is about 7ºC; these results proposed an essential characteristic of the device's operating range. Wei *et al.* [10] designed and fabricated a low-cost TMCF sensor using a commercial 0.35μm 2P4M CMOS MEMS technology. They used the configured CTD mode circuit and minimized the inconsistent sensor output due to ambient temperature variation. Wei *et al.* [11] studied the packaging effect (including two types of sensor packaging designs: S-type and E-type) on CMOS Thermo-Resistive Micro Calorimetric Flow performance sensors. They performed CFD simulations and achieved a flow regime map that the critical boundary curve for the flow separation of CMOS TMCF sensors. Lammerink *et al.* [12] presented a micro-liquid flow sensor with high sensitivity. They performed a sensor behavior analytical model. Dinh *et al.* [13] reviewed the thermoresistive effect fundamentals in metals and semiconductors. They discussed the influence of fabrication and design parameters on thermoresistive sensitivity. Balakrishnan *et al.* [14] proposed an analytical model for a released microscale heater made of 3C–SiC thin films. They showed that the potential of thermal sensors in portable applications with low power consumption (0.18mW) at 310 K. Dijkstra *et al.* [15] studied a calorimetric miniaturized flow sensor with a thermally isolated freely suspended silicon-rich silicon-nitride microchannel directly below the substrate surface. Haneveld *et al.* [16] presented the modeling, design, and realization of micromachined Coriolis mass flow sensors. They showed that the sensor measures true mass flow by water, ethanol, white gas, and argon. Nguyen [17] presented a review of the micromachined flow sensors. Van Kuijk *et al.* [18] presented a micro mechanically fabricated thermal flow sensor. They analyzed the ability of an artificial neural network to learn to discriminate between the flow velocity and flow properties. Nguyen [19] presented a unified theory for different measurement concepts of a thermal flow sensor. He

presented the experimental results of the sensor prototype. Issa *et al.* [20] introduced a theoretical model for the thermal flow sensor's response time. They found that results agree with experimental measurements and proposed the response time depends on the velocity and the sensor geometry. The evolutionary procedure has been used for material parameter identification in modeling material behavior of soft tissues by Franulović *et al.* [21]. This paper gives a detailed theoretical basis to provide inverse modeling and apply the presented method for the material models calibration and validation of the chosen parameters set. For the solution of the differential equation, different methods have been used in the researches. Ghalambazet *et al.* [22] presents an analytical solution for the buckling analysis of cantilever nanoactuators immersed in an electrolyte using the Duan-Rach Modified Adomian Decomposition Method. In another research, Noghrehabadi *et al.* [23] used the ADM–Padé technique for the electrostatic pull-in instability of nano cantilever actuators. Xu *et al.* [24] present a 3D integrated molybdenum thermoresistive micro-calorimetric flow sensor. They found that this model would be an efficient tool for the design and optimization of high-performance system-on-chip calorimetric flow sensors. Ejeian *et al.* [24] present an overview on the design and development of Microelectromechanical system (MEMS) - based flow sensors. They found that the MEMS flow sensors can be generally categorized into three main types, namely thermal sensors, piezoresistive sensors, and piezoelectric sensors. Algamili *et al.* [25] reviewed the recent developments of standard actuation and sensing mechanisms. The real-life applications, the featured principles of actuating and sensing mechanisms have been discussed.

Most studies have been based on computational fluid dynamics and experimental data, and most one-dimensional models are also presented using experimental results. Since the limited laboratory conditions lead to the extraction of results for some instances, it seems necessary to use an alternative method that can be more inclusive and, at the same time, can use materials with variable properties. The present study aims to derive a complete analytical model for sensor behavior. The current paper considers the thermal analysis and optimization of the Thermo-Resistive Micro-Calorimetric Flow Sensor using the analytical method. The energy balance equation is derived for the silicon-dioxide membrane thin layer and thermal boundary layer around the membrane in the first step. Then, silicon dioxide's temperature-dependent thermal conductivity is applied to derive differential energy balance for the membrane layer. For the derived thermal non-linear differential equation solution, the precise analytical method, the *Differential Transformation Method* (DTM), has been used. For the analytical solution confirmation, the non-linear differential equation has been solved again with the finite-element method. Sensitivity analysis has been performed to analyze the effects of operational and geometrical parameters on the considered sensor's thermal characteristics. In these sensors, the flow rate is calculated based on temperature differences on the two positions of the silicon dioxide membrane layer. The optimization has been performed at different flow velocities using a genetic algorithm to determine the optimum configuration of the thermo-resistive flow sensor. The temperature difference ratio between upstream and downstream flow has been selected as an objective function in the optimization procedure. The geometrical parameters have been chosen as the decision variables. By genetic algorithm optimization, the optimal flow sensor configuration at various flow velocities has been determined. The analytical expressions for the optimum decision variables have been derived using and curve-fitting method in the final step. The thermo-resistive micro-calorimetric flow sensor's optimum design can be achieved analytically based on flow velocity with the analytical expressions for optimum decision variables.

2. Modeling

2.1. Description of Problem

In this research, the *Thermo-Resistive Micro-Calorimetric Flow* (TMCF) sensor analysis using an analytical method, optimization based on analytical solution, and finally providing analytical correlation to find the optimal configuration is considered. *Thermo-resistive micro calorimetric flow sensor* (TMCF) is divided into open-space and channel-type categories, and in the current paper, the open-space type is considered. A schematic of a TMCF sensor is presented in Fig. 1. A TMCF sensor generally consists of a micro-heater at the center of a thin film and two thermo-resistive sensors that are symmetrically located upstream and downstream with Tu and Td's temperature, respectively. The thin film is supported by massive silicon (Si) substrate.

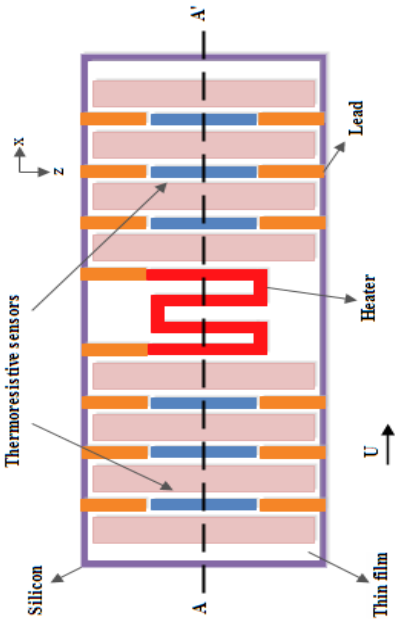

Fig. 1. Schematic of the thermo-resistive micro calorimetric flow sensor.

The temperature difference between upstream and downstream sensors is related to convective heat transfer and input flow velocity in fluid flow. Therefore, the temperature difference between the upstream and downstream sensors can be converted to an electrical signal, and mass flow measurement is performed. The geometrical parameter and sensor position dimensions and heat transfer element are shown in Fig. 2, and the detailed data are presented in Table 1. With the applied interface circuit for the upstream and downstream thermoresistive sensors, the electrical output of the TMCF sensor is monitored as a linear function of the thermal output.

Metrol. Meas. Syst., Vol. 29 (2022), No. 1
DOI: 10.24425/mms.2022.138545

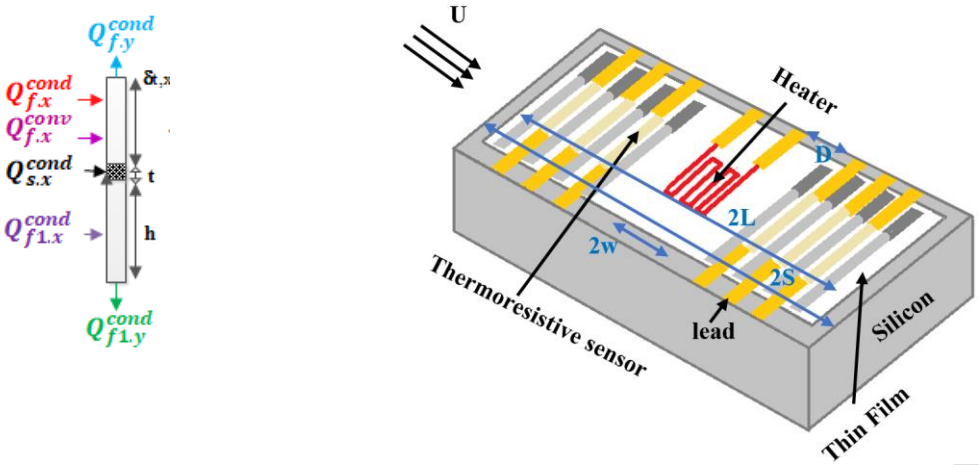

Fig. 2. Schematic of thermo-resistive micro calorimetric flow sensor dimensions.

Table. 1. Thermo-resistive micro calorimetric flow sensor dimensions [1].

Parameter	value
s(μm)	750
L(μm)	300
W(μm)	50
D(μm)	120
h(μm)	150
t(μm)	4

2.2. Energy Balance Equation

For the energy balance formulation, the lumped parameter method was employed to describe the critical behavior of TMCF sensors. For example, in the steady-state condition, the sum of the inlet convective and conductive heat fluxes in a control volume is equal to the sum of the outlet heat fluxes as follows:

$$\sum Q_{in} - \sum Q_{out} = 0 \tag{1}$$

$$Q_{f.x}^{cond} + Q_{f.x}^{conv} + Q_{s.x}^{cond} + Q_{f1.x}^{cond} = Q_{f.y}^{cond} + Q_{f1.y}^{cond} \tag{2}$$

The inlet and outlet conductive heat fluxes can be calculated as follows [2]:

$$Q_{s.x}^{cond} = k_s \frac{d^2T(x)}{dx^2} t\Delta x \tag{3}$$

$$Q_{f.x}^{cond} = \frac{1}{2} k_f \frac{d^2T(x)}{dx^2} \Delta x \delta_{t.x} \tag{4}$$

$$Q_{f1.x}^{cond} = \frac{1}{2} k_{f1} \frac{d^2T(x)}{dx^2} h\,\Delta x \tag{5}$$

$$Q_{f.y}^{cond} = k_f \frac{T(x)}{\delta_{t.x}} \Delta x \tag{6}$$

$$Q_{f1.y}^{cond} = k_{f1} \frac{T(x)}{h} \Delta x \tag{7}$$

Assuming a linear profile for flow velocity, the inlet convection heat flux for the open-space type sensor is expressed by [2]:

$$Q_{f.x}^{conv} = \frac{\rho C_p U \delta_{t.x}^2}{6\delta_x} \frac{dT(x)}{dx} \Delta x \tag{8}$$

By substituting equations (3-8) in equation (2) and considering the averaged momentum boundary layer δ and thermal boundary layer δ_t, the general one-dimensional thermal differential equation for the TMCF sensors can be presented as below[2]:

$$\frac{d}{dx}\left[\left(k_s t + \frac{1}{2}k_f \delta_t + \frac{1}{2}k_{f1} h\right)\frac{dT(x)}{dx}\right] - \rho C_P U \beta \frac{dT(x)}{dx} - \left(\frac{k_f}{\delta_t}\right)(T(x) - T_a) = 0 \tag{9}$$

In this equation, the averaged momentum boundary layer and the thermal boundary layer are considered. The variation of thermal conductivity of silicon-dioxide membrane temperature is define using equation (10) [2]:

$$k_s = k_{0.s} \times (1 + \gamma \times (T - T_a)) \tag{10}$$

After some simplification, the final non-linear thermal differential equation is derived as below [2]:

$$\frac{d}{dx}\left[\left((k_{0.s} \times \left(1 + \gamma \times (T - T_a)\right))t\right)\frac{dT(x)}{dx}\right] + \left(\frac{1}{2}k_f \delta_t + \frac{1}{2}k_{f1} h\right)\frac{d^2T}{dx^2} - \rho C_P U \beta \frac{dT(x)}{dx} - \left(\frac{k_f}{\delta_t}\right)(T(x) - T_a) = 0 \tag{11}$$

The packaged sensor type coefficient (β) is derived as below[2]:

$$\beta = \frac{\delta_t^2}{6\delta} \tag{12}$$

The averaged momentum and thermal boundary layer along the thin film for the open-space type sensor can be calculated by equation (13) and (14) [2]:

$$\delta_x = 4.64\sqrt{\frac{\mu_f (x + s)}{\rho U}} \tag{13}$$

$$\delta_t = \zeta\delta \; ; \; \zeta = \frac{1}{1.026} Pr^{-1/3}\left[1 - \left(1 - \frac{L}{s}\right)^{3/4}\right]^{1/3} \tag{14}$$

The new variable (θ) is considered for the temperature parameter [2]:

$$\theta = T - T_a \; ; \; \theta_h = T_w - T_a \tag{15}$$

The final differential equation is derived as below [2]:

$$\frac{d}{dx}\left[((k_{0.s} \times (1 + \gamma \times \theta))t)\frac{d\theta}{dx}\right] + \left(\frac{1}{2}k_f \delta_t + \frac{1}{2}k_{f1} h\right)\frac{d^2\theta}{dx^2} - \rho C_P U \beta \frac{d\theta}{dx} - \left(\frac{k_f}{\delta_t}\right)\theta = 0 \tag{16}$$

The output thermal signal of the TMCF sensor can be determined as [2]:

$$\Delta\theta = \theta(W + D) - \theta(-W - D) \tag{17}$$

By differentiating the sensor output concerning the input fluid flow velocity, the mechano-thermal sensitivity has been determined [2]:

$$S_m = \frac{d(\Delta\theta)}{dU} \tag{18}$$

2.3. Boundary condition

For the solution of equation (16), the temperature of the thin film at supporting ends is considered equal to the ambient temperature, and the microheater working temperature is assumed Tw. The temperature of the ends of the heater is used as another boundary condition based on the definition of an equation in terms of ambient temperature. These boundary conditions can be introduced with equation 19 as below [2]:

$$\theta(-L) = 0.\theta(-W) = \theta_h\,;\;\; \theta(L) = 0.\theta(W) = \theta_h \tag{19}$$

3. Method of Solution

3.1. Differential transformation method

In this section, the generalized differential transformation method developed for the non-linear differential equation's analytical solution is presented. For example, the generalized differential transformation of the *n*-th derivative of function *f*(*x*) is as follows:

$$F_\alpha(k) = \frac{1}{\Gamma(\alpha k+1)}\left[(D_{x_0}^{\alpha})^k f(x)\right]_{x=x_0} \tag{20}$$

And the generalized differential inverse transformation of $F_\alpha(k)$ is defined as:

$$f(x) = \sum_{k=0}^{\infty} F_\alpha(k)(x-x_0)^{\alpha k} \tag{21}$$

The fundamental mathematical operations used in the generalized differential transformation method are listed in Table. 2.

Table 2. The fundamental operations in Generalized Differential Transform Method [27].

Original function	Transformed function
$\boldsymbol{f(x) = g(x) \pm h(x)}$	$\boldsymbol{F_\alpha(k) = G_\alpha(k) \pm H_\alpha(k)}$
$\boldsymbol{f(x) = ag(x)}$	$\boldsymbol{F_\alpha(k) = aG_\alpha(k)}$
$\boldsymbol{f(x) = g(x) * h(x)}$	$\boldsymbol{F_\alpha(k) = \sum_{l=0}^{k} G_\alpha(l)H_\alpha(k-l)}$
$\boldsymbol{f(x) = g_1(x)g_2(x)g_2(x)\ldots \cdot g_{n-1}(x)g_n(x)}$	$\boldsymbol{F_\alpha(k) = \sum_{k_{n-1}=0}^{k}\ \sum_{k_{n-2}=0}^{k_{n-1}} \cdots \sum_{k_2=0}^{k_3}\ \sum_{k_1=0}^{k_2} G_1(k_1)G_2(k_2-k_1)\ldots G_{n-1}(k_{n-1}-k_{n-2})G_n(k-k_{n-1})}$
$\boldsymbol{f(x) = D_{x_0}^{\alpha} g(x)}$	$\boldsymbol{F_\alpha(k) = \frac{\Gamma(\alpha(k+1)+1)}{\Gamma(\alpha k+1)} G_\alpha(k+1)}$
$\boldsymbol{f(x) = (x-x_0)^{\gamma}}$	$\boldsymbol{F_\alpha(k) = \delta\left(k-\frac{\gamma}{\alpha}\right).\, where\ \delta(k) = \begin{cases} 1\ if\ k=0 \\ 0\ if\ k\neq 0 \end{cases}}$
$\boldsymbol{f(x) = D_{x_0}^{\beta} g(x)}$	$\boldsymbol{F_\alpha(k) = \frac{\Gamma(\alpha(k)+\beta+1)}{\Gamma(\alpha k+1)} G_\alpha(k+\frac{\beta}{\alpha})}$
$\boldsymbol{\int_{x_0}^{x} g(t)dt}$	$\boldsymbol{F_\alpha(k) = \frac{(G_\alpha(k-\frac{1}{\alpha}))}{\alpha k}.\, where\ k \geq 1/\alpha}$

3.2. Finite Element method

For the analytical solution confirmation, the FlexPDE software package has been chosen as the numerical solving tool. FlexPDE is a general-purpose software package for obtaining numerical solutions to ordinary and partial differential equations based on the Finite Element Method. FlexPDE uses an Adaptive Mesh Refinement method. Once the initial mesh is constructed, FlexPDE estimates the solution error and refines the mesh as necessary to meet the

target accuracy. Cells created by this adaptive refinement process can later be remerged. FlexPDE also automatically recognizes when a problem is non-linear and modifies its strategy accordingly. The solution method tries to fall down the gradient of an energy functional until minimum power is achieved (*i.e.*, the functional gradient goes to zero). The default strategy implemented in FlexPDE is frequently sufficient to determine a solution without user intervention.

4. The solution of the differential equation

This section applies the differential transformation to the governed non-linear differential equation (equation (16)). Based on DTM principles, the final transformed differential equation can be presented as below:

$$\begin{aligned}\sum_{n=0}^{k}(k+1-n)(k+2-n)\theta_{k+2-n}\theta_k+\sum_{n=0}^{k}(k+1-n)\theta_{k+1-n}(n+1)\theta_{n+1}\\ +A(k+1)(k+2)\theta_{k+2}\\ +B\sum_{n=0}^{k}(k+1-n)(k+2-n)\theta_{k+2-n}G_n\\ -C\sum_{n=0}^{k}\sum_{m=0}^{n}(k+1-n)\theta_{k+1-n}H_{n-m}\delta_m\\ -DD\sum_{n=0}^{k}(k+1-n)\theta_{k+1-n}H_n-E\sum_{n=0}^{k}\theta_{k-n}H_n-F\theta_k=0\end{aligned} \tag{22}$$

where

$$\begin{aligned}A=\left(\frac{1}{\beta}+\frac{k_{f1}h}{2k_0\beta t}\right).B=\frac{2.32k_f\zeta}{k_0\beta t}.C=\frac{0.7734\zeta^2C_p\mu_f}{k_0\beta t}.DD=Cs.E\\ =\frac{0.2155172414k_f}{k_0\beta t\zeta}.F=\frac{k_{f1}}{k_0\beta th}\end{aligned} \tag{23}$$

G and H are the differential transformation of $\sqrt{at+b}$ and $\frac{1}{\sqrt{at+b}}$ respectively. The DTM of boundary condition can be evaluated as below:

$$\theta_0=aa,\ \theta_1=bb \tag{24}$$

Where aa and bb are auxiliary parameters and are calculated at the final step, with the solution procedure, the required coefficients are calculated as below:

$$\theta_2=\frac{1}{2}\frac{-bb^2\sqrt{b}+C\ bb+DD\ bb+E\ aa+F\ aa\sqrt{b}}{aa\sqrt{b}+A\sqrt{b}+B\ b} \tag{25}$$

$$\begin{aligned}\theta_3=-\frac{1}{12}(&2C\ bb\ a\ B\ b+2\ DD\ bb\ a\ B\ b+2E\ aa\ a\ B\ b+B\ b^{3/2}a\ F\ aa+C\ bb\ a\ aa\sqrt{b}\\ &+C\ bb\ a\ A\sqrt{b}+DD\ bb\ a\ aa\sqrt{b}+DD\ bb\ a\ A\sqrt{b}-2E\ bb\ b^2B\\ &+E\ aa\ a\ A\sqrt{b}-2F\ bb\ b^{5/2}B+4bb\ b^{3/2}\ E\ aa+4\ bb\ b^2\ F\ aa\\ &-B\ b^{3/2}\ a\ bb^2-4\ C\ b\ DD\ bb-2C\ b\ E\ aa-2Cb^{3/2}\ F\ aa\\ &-2DD\ b\ E\ aa-2DD\ b^{3/2}\ F\ aa-2E\ bb\ b^{3/2}A+E\ aa^2a\sqrt{b}\\ &-2F\ bb\ b^2A+8\ bb^2b^{3/2}C+8\ bb^2b^{3/2}DD-2bC^2bb-2b\ DD^2bb\\ &-6bb^3b^2)/(bb\ b^{5/2}B+2b^{5/2}A\ B+bb\ b^2aa+bb\ b^2\ A+b^2\ A\ aa\\ &+Bb^{5/2}aa+B^2b^3+b^2A^2)\end{aligned} \tag{26}$$

5. Optimization of the sensing element position

Achieving an optimal design to maximize sensor measurement accuracy is one of the most critical issues in designing thermo-resistive sensors. Increasing the accuracy of the sensors requires increasing the temperature difference .This paper aims to achieve an optimal analytical design to guarantee the maximum temperature difference in the thermo-resistive sensor. For this purpose, the genetic algorithm optimization method (optimization toolbox in MATLAB) [28] has been used. The objective function is the temperature difference between the upstream and downstream flow sensors that should be maximized:

$$Objective\ Function = \frac{\theta_{upper} - \theta_{lower}}{\theta_h} \tag{27}$$

The decision variables are the geometric parameter listed in Table 3.

Table 3. the decision variable used in the optimization procedure.

Parameter	Symbol	Range
Sensor distance from the heater	D	100-150 μm
Partially heated length	L	200-400 μm
Heater temperature	Th	30-70 K
Length of heater	W	30-70 μm
cavity height	h	100-200 μm
Length of the bare TMCF sensor chip	s	600-800 μm

The main tuning parameters for the genetic algorithm optimization are as below:

- Population size: 700
- Maximum number of generations: 400
- Probability of crossover: 75(%)
- Probability of mutation: 1(%)
- Number of crossovers: point 2
- Selection process: Tournament (size= 2)

The optimization process for different flow velocity values (U) is performed to have a flexible optimal design. Finally, an analytical correlation for the optimal geometric parameters in flow velocity is created using the curve fitting.

6. Results and Discussion

The comparison of the current analytical result, numerical solution (FlexPDE), and reference [2] are shown in Fig. 3. The authors stated that the one-dimensional model results were the same as the experimental results in this reference. The comparison shows that the analytical results have excellent agreement with the numerical solution and reference [2]. Also, the evaluation of modeling error in Table. 3 shows that the model error rate is in a suitable range. Furthermore, the result shows that the output temperature difference ($\Delta\theta$) increased with the fluid flow velocity increment. Therefore the 1D simulated model of TMCF sensors with a fitting function agrees with the numerical solution and previous studies. The device geometry and parameters are considered the same as the reference for comparison. Therefore, the 1D model with a correction fitting function can be considered as a semi-empirical TMCF model.

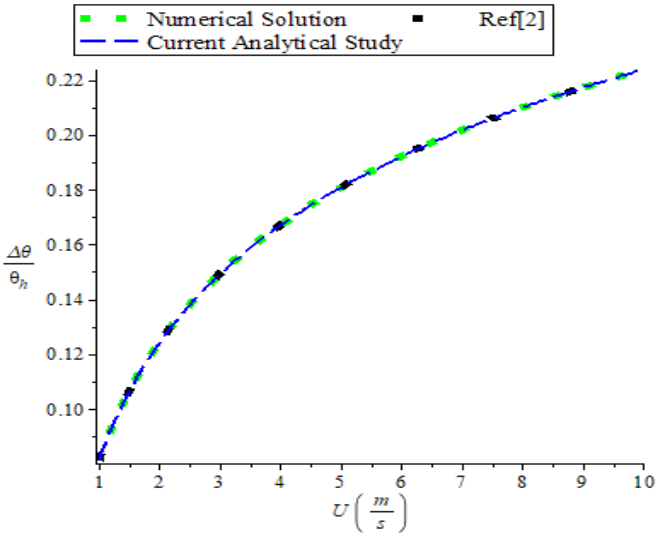

Fig. 3. Thermo-resistive micro calorimetric flow sensor modeling verification.

Table. 3. Comparison of analytical and numerical solution.

U	Analytical Solution	Numerical Solution	Relative Error	U	Analytical Solution	Numerical Solution	Relative Error
0.5	0.052605762	0.052702202	0.183	**5.5**	0.185516498	0.185611463	0.051
1	0.082161081	0.082174754	0.017	**6**	0.191453366	0.191546944	0.049
1.5	0.103503457	0.103559132	0.054	**6.5**	0.197159947	0.197227616	0.034
2	0.119959534	0.119985286	0.021	**7**	0.202374453	0.202461821	0.043
2.5	0.133456978	0.133463549	0.005	**7.5**	0.206770241	0.20685421	0.041
3	0.145159343	0.145201262	0.029	**8**	0.210801799	0.210862036	0.029
3.5	0.15992914	0.159942336	0.008	**8.5**	0.214781131	0.214781474	0.000
4	0.162628312	0.162647339	0.012	**9**	0.218526368	0.218529448	0.001
4.5	0.171170781	0.171237896	0.039	**9.5**	0.222249377	0.222252395	0.001
5	0.179418969	0.179447689	0.016	**10**	0.225930261	0.225947399	0.008

The variation of sensitivity (S_m) with the fluid flow velocity is presented in Fig. 4. The result shows that sensitivity decreased with the fluid flow velocity increment, and this status indicates a trade-off between the output amplitude and sensitivity. Thus, the sensitive TMCF sensor can be achieved at a small input flow, allowing micro calorimetric flow sensors to be applied in low flow velocity measurements.

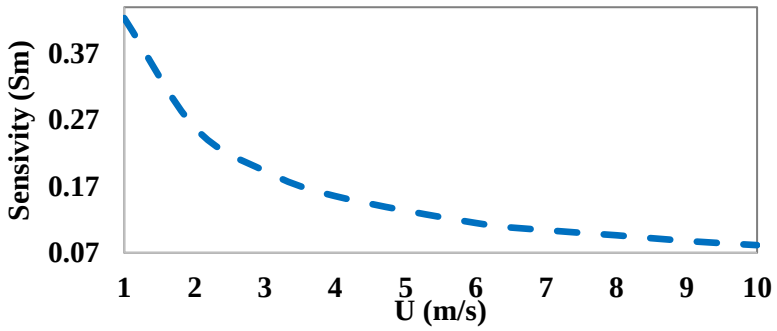

Fig. 4. Thermo-resistive micro calorimetric flow sensor sensitivity.

Investigating the effect of different parameters on sensor performance show that the film thickness, cavity height, and heater-sensors distance have the most impact on temperature difference and therefore have more effect on sensor sensitivity. On the other hand, based on equation 8 the convective heat transfer depends on the velocity and working fluid property. And by changing the velocity of the fluid, the convective heat transfer shows its effect on the temperature distribution in the sensor. Therefore, in this section, the impact of these parameters is investigated by several figures. Fig. 5 presents that a smaller film thickness can be led to higher $\frac{\Delta\theta}{\theta_h}$ in the TMCF sensor. Because with increasing the film thickness, the heat leakage is increased by increasing the conduction heat transfer, and as a result, the temperature decreases. It should be noted that complex technology is required to fabricate these thin films. Fig. 5 shows that the temperature difference increases with the velocity increment at the different film thicknesses. Because the convective heat transfer from the free stream flow is increased. Therefore, at lower velocities, the accuracy of the measurements will be higher.

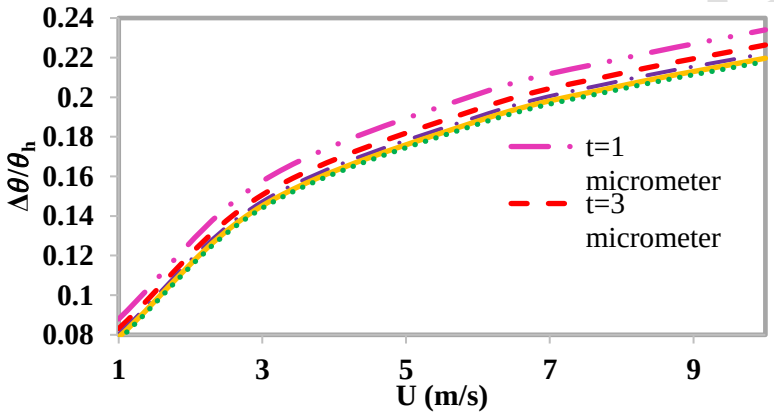

Fig. 5. The effect of thin-film thickness on Thermo-resistive micro calorimetric flow sensor $\frac{\Delta\theta}{\theta_h}$.

As shown in Fig. 6, the temperature difference does not change significantly at different cavity heights (at the bottom) at the specific velocity. Because increasing the cavity heights (h) increases the conduction heat transfer in the x-direction and decreases the conductive heat transfer in the y-direction. Examination of the governing equations (Equation 2) shows that the only heat transfer terms affected by cavity height are $Q_{f1.x}^{cond}$ and $Q_{f1.y}^{cond}$ (Equations 5 and 7). Further studies show that changes in cavity height have an increasing effect on $Q_{f1.x}^{cond}$ and a decreasing effect on $Q_{f1.y}^{cond}$. Due to these factors, the cavity height variations do not significantly affect the temperature distribution. However, the investigation at different velocities shows that temperature difference is increased with the velocity variations at the channel's specified heights.

In Fig. 7, the temperature difference ratio ($\frac{\Delta\theta}{\theta_h}$) was evaluated at different velocities and heater/sensor distance. Fig. 7 shows that the temperature difference decreases with heater/sensor distance increment at a constant velocity. So with increasing D, the accuracy of sensor measurement improves. However, results show that increasing the flow velocity at different heater/sensor distances increases the temperature difference ratio. Therefore, increasing the flow velocity will reduce the accuracy of the sensor measurement.

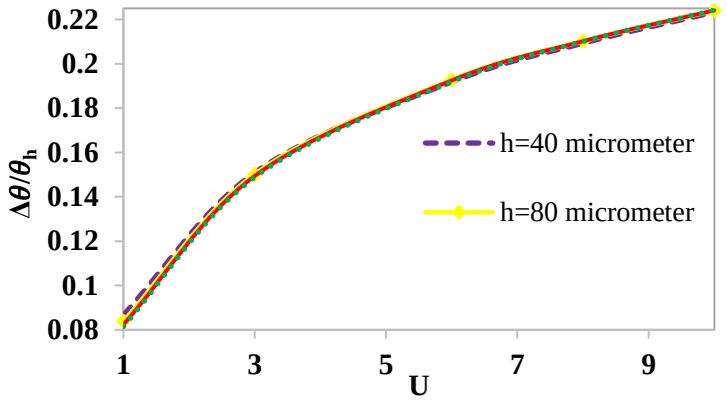

Fig. 6. The effects of bottom cavity height h on the sensor's temperature difference ($\frac{\Delta\theta}{\theta_h}$).

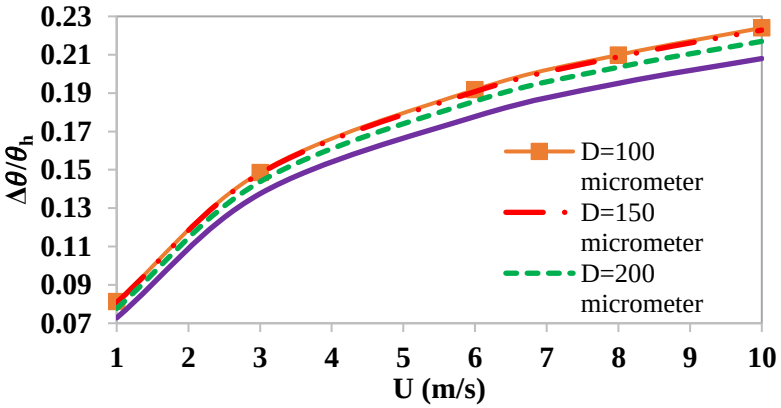

Fig. 7. The effects of distance between the heater and the sensing elements on the sensor's temperature difference ($\frac{\Delta\theta}{\theta_h}$).

To determine the optimum thermo-resistive sensor configuration, an optimization process using a genetic algorithm has been performed at different flow velocities. The genetic algorithm optimization process is performed for different fluid flow velocities (as an input parameter) to achieve maximum sensitivity, and optimal geometry is determined for each velocity. The results of the optimization are shown in Table. 4.

Table. 4 the result of thermo-resistive sensor optimization

U (m/s)	D (μm)	L (μm)	$\theta_h(k)$	w (μm)	h (μm)	s(μm)	t(μm)
1	107.27	287.68	45.53	50.12	197.74	784.19	4.66
2	150.00	200.00	63.41	68.68	199.82	823.64	4.30
3	150.00	200.00	30.75	69.76	197.93	850.00	6.00
4	150.00	200.00	40.82	70.00	167.93	850.00	5.27
5	149.25	209.48	53.62	69.28	136.45	821.71	4.04
6	149.31	242.40	54.00	69.38	192.50	610.83	4.55
7	146.21	202.19	64.52	69.47	184.63	838.09	3.06
8	144.48	225.87	67.97	62.78	150.56	738.84	4.11
9	150.00	241.38	30.75	69.82	200.00	667.38	2.00
10	146.60	201.46	53.44	68.91	189.63	836.32	4.09

The optimization results (data bank) have developed analytical correlations using the curve-fitting method. As a result, the optimum geometrical configuration of the thermo-resistive flow sensor can be derived simply at any velocity, using these analytical correlations.

$$D = -e^{-8}U^6 + 5e^{-7}U^5 - 7e^{-6}U^4 + 5e^{-5}U^3 - 0.0002U^2 + 0.0003U - 8e^{-5} \quad (28)$$

$$L = -2e^{-8}U^6 + 6e^{-7}U^5 - 7e^{-6}U^4 + 3e^{-5}U^3 - 1e^{-5}U^2 - 0.0002U + 0.0004 \quad (29)$$

$$W = -8e^{-9}U^6 + 3e^{-7}U^5 - 4e^{-6}U^4 + 2e^{-5}U^3 - 9e^{-5}U^2 + 0.0002U - 4e^{-5} \quad (30)$$

$$h = -2e^{-8}U^6 + 7e^{-7}U^5 - 9e^{-6}U + 7e^{-5}U^3 - 0.0002U^2 + 0.0004U - e^{-5} \quad (31)$$

$$s = 2e^{-7}U^6 - 7e^{-6}U^5 + 9e^{-5}U^4 - 0.0005U^3 + 0.0016U^2 - 0.0021U + 0.0018 \quad (32)$$

$$\theta_h = 0.0013U^6 + 0.059U^5 - 2.2292U^4 + 23.837U^3 - 105.99U^2 + 193.23U^1 - 62.212 \quad (33)$$

7. Conclusion

The analytical method was applied to analyze and optimize the thermo-resistive micro-calorimetric flow sensor in the current paper. The differential energy balance equation, including convection/conduction terms and temperature-dependent thermal conductivity, is derived in the first step. Then, the famous analytical method, the so-called differential transformation method, has been used for an analytical solution. The sensitivity analysis using an analytical solution shows that the sensor sensitivity was increased with flow velocity decrement, film thickness decrement, and heater-sensor distance increment. In the final step, the geometrical optimization of the thermo-resistive sensor has been performed using the genetic algorithm method at different flow velocities. The different analytical correlations have been presented based on optimization data (at different velocities) for the optimum geometrical parameter. Using these analytical geometrical parameters, an optimum configuration can be specified analytically at any flow velocity.

Nomenclature

2s (μm)	Length of the bare TMCF sensor chip	u	Upstream
2L (μm)	Partially heated length	d	Downstream
2W (μm)	Length of heater	Subscript	
D (μm)	Sensor distance from the heater	h	Heater
h (μm)	cavity height	f	moving fluid on the top of the thin film
T (K)	Temperature	f1	fluid in the cavity
t (μm)	Thin-film thickness	s	thin film
K (W/mK)	Thermal conductivity	w	the working temperature of the microheater
U (m/s)	Flow velocity	Greek letters	
S_m (K/(m/s))	Sensitivity	δ	momentum boundary layer
cond	Conduction heat transfer	δ_t	thermal boundary layer
conv	Convection heat transfer	θ	Temperature variable change
Pr	Prandtl Number	μ	Viscosity

References

[1] Xu, W., Song, K., Ma, S., Chiu, Y., & Lee, Y. K. (2014, October). One dimensional model of thermoresistive micro calorimetric flow sensors for gases and liquids considering Prandtl number effect. In *Conf. on Miniaturized Systems for Chemistry and Life Sciences (MicroTAS2014)* (pp. 2333-5).

[2] Xu, W., Song, K., Ma, S., Gao, B., Chiu, Y., & Lee, Y. K. (2016). Theoretical and experimental investigations of thermoresistive micro calorimetric flow sensors fabricated by CMOS MEMS technology. *Journal of Microelectromechanical Systems*, *25*(5), 954-962. https://doi.org/10.1109/JMEMS.2016.2596282

[3] Silvestri, S., & Schena, E. (2012). Micromachined flow sensors in biomedical applications. *Micromachines*, *3*(2), 225-243. https://doi.org/10.3390/mi3020225

[4] Shaun, F., Sarkar, S., Marty, F., Poulichet, P., Cesar, W., Nefzaoui, E., & Bourouina, T. (2018). Sensitivity optimization of micro-machined thermo-resistive flow-rate sensors on silicon substrates. *Journal of Micromechanics and Microengineering*, *28*(7), 074002. https://doi.org/10.1088/1361-6439/aab6bd

[5] Xu, W., Gao, B., Ahmed, M., Duan, M., Wang, B., Mohamad, S., Bermak, A. & Lee, Y. K. (2017, January). A wafer-level encapsulated CMOS MEMS thermoresistive calorimetric flow sensor with integrated packaging design. In *2017 IEEE 30th International Conference on Micro Electro Mechanical Systems (MEMS)* (pp. 989-992). IEEE. https://doi.org/10.1109/MEMSYS.2017.7863577

[6] Xu, W., Ma, S., Wang, X., Chiu, Y., & Lee, Y. K. (2019). A CMOS-MEMS thermoresistive micro calorimetric flow sensor with temperature compensation. *Journal of Microelectromechanical Systems*, *28*(5), 841-849. https://doi.org/10.1109/JMEMS.2019.2928317

[7] Kohl, F., Beigelbeck, R., Loschmidt, P., Kuntner, J., & Jachimowicz, A. (2006). *FEM-based analysis of micromachined calorimetric flow sensors* (pp. 1215-1218). IEEE. https://doi.org/10.1109/ICSENS.2007.355846

[8] Dumstorff, G., Brauns, E., & Lang, W. (2015). Investigations into packaging technology for membrane-based thermal flow sensors. *Journal of Sensors and Sensor Systems*, *4*(1), 45-52. https://doi.org/10.5194/jsss-4-45-2015

[9] Arevalo, A., Byas, E., & Foulds, I. G. (2013, October). Simulation of thermal transport based flow meter for microfluidics applications. In *2013 COMSOL Conference, Rotterdam, Holland*.

[10] Xu, W., Gao, B., Ma, S., Zhang, A., Chiu, Y., & Lee, Y. K. (2016, January). Low-cost temperature-compensated thermoresistive micro calorimetric flow sensor by using 0.35 μm CMOS MEMS technology. In *2016 IEEE 29th International Conference on Micro Electro Mechanical Systems (MEMS)* (pp. 189-192). IEEE. https://doi.org/10.1109/MEMSYS.2016.7421590

[11] Xu, W., Gao, B., Lee, Y. K., & Chiu, Y. (2016, April). Packaging effect on the flow separation of CMOS thermoresistive micro calorimetric flow sensors. In *2016 IEEE 11th Annual International Conference on Nano/Micro Engineered and Molecular Systems (NEMS)* (pp. 62-65). IEEE. https://doi.org/10.1109/NEMS.2016.7758201

[12] Lammerink, T. S., Tas, N. R., Elwenspoek, M., & Fluitman, J. H. (1993). Micro-liquid flow sensor. *Sensors and actuators A: Physical*, *37*, 45-50. https://doi.org/10.1016/0924-4247(93)80010-E

[13] Dinh, T., Phan, H. P., Qamar, A., Woodfield, P., Nguyen, N. T., & Dao, D. V. (2017). Thermoresistive effect for advanced thermal sensors: Fundamentals, design considerations, and applications. *Journal of Microelectromechanical Systems*, *26*(5), 966-986. https://doi.org/10.1109/JMEMS.2017.2710354

[14] Balakrishnan, V., Dinh, T., Phan, H. P., Kozeki, T., Namazu, T., Dao, D. V., & Nguyen, N. T. (2017). Steady-state analytical model of suspended p-type 3C–SiC bridges under consideration of Joule heating. *Journal of Micromechanics and Microengineering*, *27*(7), 075008. https://doi.org/10.1088/1361-6439/aa7180

[15] Dijkstra, M., de Boer, M. J., Berenschot, J. W., Lammerink, T. S., Wiegerink, R. J., & Elwenspoek, M. (2008). Miniaturized thermal flow sensor with planar-integrated sensor structures on semicircular surface channels. *Sensors and Actuators A: Physical*, *143*(1), 1-6. https://doi.org/10.1016/j.sna.2007.12.005

[16] Haneveld, J., Lammerink, T. S., de Boer, M. J., Sanders, R. G., Mehendale, A., Lötters, J. C., ... & Wiegerink, R. J. (2010). Modeling, design, fabrication and characterization of a micro Coriolis mass flow sensor. *Journal of Micromechanics and Microengineering*, *20*(12), 125001. https://doi.org/10.1088/0960-1317/20/12/125001

[17] Nguyen, N. T. (1997). Micromachined flow sensors—a review. *Flow Measurement and Instrumentation*, *8*(1), 7-16. https://doi.org/10.1016/S0955-5986(97)00019-8

[18] van Kuijk, J., Lammerink, T. S. J., De Bree, H. E., Elwenspoek, M., & Fluitman, J. H. J. (1995). Multi-parameter detection in fluid flows. *Sensors and Actuators A: Physical*, *47*(1-3), 369-372. https://doi.org/10.1016/0924-4247(94)00923-6

[19] Nguyen, N. T. (2005). A novel thermal sensor concept for flow direction and flow velocity. *IEEE Sensors Journal*, *5*(6), 1224-1234. https://doi.org/10.1109/JSEN.2005.858924

[20] Issa, S., Sturm, H., & Lang, W. (2011). Modeling of the response time of thermal flow sensors. *Micromachines*, *2*(4), 385-393. https://doi.org/10.3390/mi2040385

[21] Franulović, M., Marković, K., & Trajkovski, A. (2021). Calibration of material models for the human cervical spine ligament behaviour using a genetic algorithm. *Facta Universitatis, Series: Mechanical Engineering*.

[22] Ghalambaz, M., Ghalambaz, M., & Edalatifar, M. (2015). Buckling analysis of cantilever nanoactuators immersed in an electrolyte: a close form solution using Duan-Rach modified Adomian decomposition method. *Journal of Applied and Computational Mechanics*, *1*(4), 207-219. https://dx.doi.org/10.22055/jacm.2015.12024

[23] Noghrehabadi, A., Ghalambaz, M., & Ghanbarzadeh, A. (2012). A new approach to the electrostatic pull-in instability of nanocantilever actuators using the ADM–Padé technique. *Computers & Mathematics with Applications*, *64*(9), 2806-2815. https://doi.org/10.1016/j.camwa.2012.04.013

[24] Xu, W., Wang, B., Duan, M., Ahmed, M., Bermak, A., & Lee, Y. K. (2019). A three-dimensional integrated micro calorimetric flow sensor in CMOS MEMS technology. *IEEE Sensors Letters*, *3*(2), 1-4. https://doi.org/10.1109/LSENS.2019.2893151

[25] Ejeian, F., Azadi, S., Razmjou, A., Orooji, Y., Kottapalli, A., Warkiani, M. E., & Asadnia, M. (2019). Design and applications of MEMS flow sensors: A review. *Sensors and Actuators A: Physical*, *295*, 483-502. https://doi.org/10.1016/j.sna.2019.06.020

[26] Algamili, A. S., Khir, M. H. M., Dennis, J. O., Ahmed, A. Y., Alabsi, S. S., Hashwan, S. S. B., & Junaid, M. M. (2021). A review of actuation and sensing mechanisms in MEMS-based sensor devices. *Nanoscale Research Letters*, *16*(1), 1-21. https://doi.org/10.1186/s11671-021-03481-7

[27] Babaelahi, M., Ganji, D. D., & Joneidi, A. A. (2010). Analysis of velocity equation of steady flow of a viscous incompressible fluid in channel with porous walls. *International journal for numerical methods in fluids*, *63*(9), 1048-1059. https://doi.org/10.1002/fld.2114

[28] Sayyaadi, H., & Babaelahi, M. (2010). Exergetic optimization of a refrigeration cycle for re-liquefaction of LNG boil-off gas. *International Journal of Thermodynamics*, *13*(4), 127-133.